INTERNATIONAL JOURNAL OF CONSERVATION SCIENCE
ISSN: 2067-533X Volume 11, Special Issue 1, 2020: 345-352 www.ijcs.uaic.ro

STATISTICAL APPROACH FOR EQUIVALENT DOSE DETERMINATION IN HISTORICAL MORTARS DATING

Giuseppe STELLA, Stefania PASQUALE*, Anna Maria GUELI

PH3DRA labs, Department of Physics and Astronomy "Ettore Majorana" of Catania University & INFN CHNEt sez Catania– via S. Sofia 64 – 95123 Italy.

Abstract

A methodological study aimed to evaluate the bleaching degree of quartz fractions extracted from historical mortars is presented. Equivalent Dose (ED) measurements on small aliquots of two different quartz fraction, inclusion (90 µm<Ø<150 µm) and coarse grain (180 µm<Ø<212 µm), were performed by optically stimulated luminescence using single aliquot regeneration procedure. In order to choose the more suitable age model to be used, the bleaching degree was studied through a deep statistical approach using ED frequency distribution, Q-Q plot and Shapiro-Wilk normality test. The results show that ED from coarse grain could be statistically associated to normal distribution and then Central Age Model (CAM) can be used for Archaelogical dose calculation. The quartz inclusion data don't follow a normal distribution and then Minimum Age Model (MAM) is more appropriate. Archaelogical dose results obtained in two different age models were in good agreement.

Keywords*: Normality test; Age model; Historical mortar dating; OSL measurements.*

Introduction

In last years, the OSL is becoming one of the most used methodology to date mortars coming from historical buildings [1-11]. Because OSL is a destructive technique that implies the sampling of mortar from the historical fabric, it is becoming fundamental optimize the procedures and the protocols aimed at calculating the equivalent dose and thus the age from small quantities of collected samples. In this context, the presented study proposes a methodological approach based on statistics for improving the evaluation of the bleaching degree that affects the accuracy of the equivalent dose calculation.

The evaluation of bleaching degree related to the granulometry of the extracted and measured quartz from historical mortar has been studied [1-11]. Goedicke [4] has discussed all problems related to mortar dating including the most suitable method of equivalent dose and dose rate determination, showing all issues known for sediments: for instance, partial bleaching, low signal and slow decay. Other authors have dated mortars by OSL techniques using a mixed quartz-enriched polymineral phase enriched in quartz with excellent results [3, 6, 11]. However, in the case of fine grain fraction deposited on aliquots, the high number of grains tends to average all signals and to reduce the dispersion between aliquots. For this reason, the deviation from a normal distribution is much less observable. In this case, the bleaching degree is indicative but not exhaustive. Recent studies on mortar dating demonstrate that mortar aggregate can contain a sufficient number of well-bleached quartz grains and this represents a real potential for dating the mortars by Single Grain OSL (SG-OSL) [7-10].

* Corresponding author: stefania.pasquale@ct.infn.it

The evaluation of the degree of bleaching determines the choice of the Age models [12]: the Central Age Model (CAM) [13] and the Minimum Age Model (MAM) [13-14].

In this work, four mortars were sampled from already dated "Terme dell'Indirizzo" [15-16], the best-preserved thermal baths in the Roman Empire located in the historic center of Catania (Italy). Bleaching degree was studied for quartz fractions of two different size extracted and measured in small aliquot through OSL. The choice of the age model was based on the results deriving from qualitative and quantitative statistical analysis such as ED frequency distribution; Q-Q plot and Shapiro-Wilk normality test [17-18].

Experimental

Chemical-physical preparation of the samples

In order to exclude the natural alpha and beta contribution from the environment, the two external millimetres of each mortar were eliminated and then the samples were crushed in an agate mortar. After a first sieving, aimed to select grains less than 300 microns, the samples were treated with hydrogen peroxide (35% H_2O_2) and with hydrochloric acid (10% HCl) to remove respectively the organic and the carbonate components.

The pure quartz fraction was extracted using a densitometric separation method with sodium polytungstate solutions of fixed density.

The obtained quartz fraction was divided into two granulometric ranges by sieving: Quartz Inclusion (QI) (90 μm <Ø <150 μm) and Coarse Grain (CG) (180 μm <Ø <212 μm). Further etching with fluoridric acid (40% HF) was done to eliminate natural alpha dose contribution from the sample followed by hydrochloric acid (10% HCl) to remove any acid-soluble fluorides formation [19-23].

Methods

OSL mesurements

In order to calculate the equivalent dose, the QI and CG quartz powder fractions were deposited on discs and optically stimulated luminescence measurements were performed applying Single Aliquot Regeneration (SAR). The feldspars contamination was previously checked by IR stimulation on some small aliquots of each sample [24].

The first SAR cycle consists in the reading of natural luminescence obtained by blue LEDs (470 ± 30 nm at ~30 mW/cm^{-2}). Then calibrated beta source (^{90}Sr/^{90}Y with dose rate of 6 Gy/min) irradiation was delivered on the aliquots and the luminescence signal was recorded. In addition, repeated irradiation cycles with increasing doses were delivered and the luminescence was registered. Each step is followed by a beta irradiation that corresponds to the same dose value given in the first cycle and the related luminescence reading in order to evaluate changes in quartz sensitivity during the regeneration phases.

The equivalent dose, that is the dose value obtained by artificial beta irradiation corresponding to the same natural luminescence signal by natural beta and gamma radiations, is calculated [25-26].

The measurements are carried out by semi-automated Risoe reader TL-DA-15 with EMI 9235QA photomultiplier and a Hoya U340 optical filter [27-29].

Statistical analysis for ED distribution

The evaluation of bleaching degree related to the extracted quartz inclusion from historical mortar is very important in order to chose the best procedure of data elaboration and to evaluate the reliability of the results. In this article, the statistical analysis of the ED values, aimed at verifying the bleaching degree of the obtained data, is useful to select the age model between the MAM and the CAM.

The application of CAM required that the data are well-modelled by a normal distribution and this is linked to well-bleached degree. Vice versa, the non normal distribution is linked to partial bleached degree. MAM assumes that the sample is composed of two or more populations of grains with different bleaching, leading to a multimodal distribution of ED. The

ED values result from a non normal distribution, where the lower truncation point corresponds to the average log value of the fully bleached grains.

The first approach for normal distribution determination is the graphical method. In particular, in this work, for each sample and for each granulometric fraction, frequency distribution graphed with histogram and Quantile-Quantile (Q-Q) plots were used. The frequency distribution shows the different measurement categories and the number of observations in each category. The range is divided into arbitrary intervals called bins. For the choice of the number of bins, the Sturges rule was used. It is derived from a binomial distribution assuming an approximately normal distribution. The number of bins is given by the formula:

$$k = 1 + log_2 n \tag{1}$$

where n is the number of the events observed [30].

The Q-Q plot is a graphical tool to assess if a set of data plausibly comes from some theoretical distribution such as a Normal. A Q-Q plot is a scatterplot obtained by plotting two sets of quantiles against one another. If both sets of quantiles came from the same distribution, we should see the points forming a line that is roughly straight.

For quantitative test, Shapiro-Wilk normality test was used [31]. Shapiro and Wilk proposed the W test based on the statistic:

$$W = \frac{\left(\sum_{i=1}^{n} a_i X_{(i)}\right)^2}{\sum_{i=1}^{n}(X_i - \bar{X})^2} \tag{2}$$

where $X_{(1)} \leq X_{(2)} \leq \cdots \leq X_{(n)}$ are the ordered X_i ED values of a sample and a_i is the statistical tabulated coefficient.

Assuming that the expected value μ, named μ_0, is known, the null hypothesis (H_0) has to be tested:

$$H_0 = X \sim N(\mu_0, \sigma^2) \tag{3}$$

The application of Shapiro and Wilk's technique gives the statistic

$$W_0 = \frac{\left(\sum_{i=1}^{n} a_i X_{(i)}\right)^2}{\sum_{i=1}^{n}(X_i - \mu_0)^2} \tag{4}$$

The null hypothesis (3) is rejected when $W_0 < W(\alpha, n)$, where $W(\alpha, n)$ is the critical tabulated value at the chosen significance level.

Normality tests calculate the probability that the sample was drawn from a normal population. Statistical normality tests are more precise since actual probabilities are calculated (p-value calculated) related to choice $p_c = 0.05$. P-value calculated > 0.05 indicates a normal distribution of the data while P-value calculated < 0.05 means that the data distribution are non-normal.

In order to determine the best representation of the true archaeological ED, based on the results obtained by Shapiro Wilk's tests, the more appropriate Age Model was chosen using Radial Plot that are bivariate (x_j,y_j) scatterplots where:

$$\begin{cases} x_i = 1/\sigma(z_j) \\ yi = (z_j - z_0)/\sigma(z_j) \\ 1 \leq j < n \end{cases} \tag{5}$$

with z_j is a transformation of some data and $s(z_j)$ the corresponding measurement uncertainty. For example, if $z_j=\log(t_j)$ then $\sigma(z_j) = \sigma(t_j)/t_j$. z_0 is the central value (weighted mean). The horizontal distance along x-axis is a measure if the precision [32].

Results and discussion

ED frequency distribution

The first step consists in the plot of the dose histogram to observe, through the form of the frequency distribution, the bleaching degree of the grains. An example of ED frequency

distribution for both the QI and CG fraction of the IM6 sample are shown in the Figures 1 and 2 respectively.

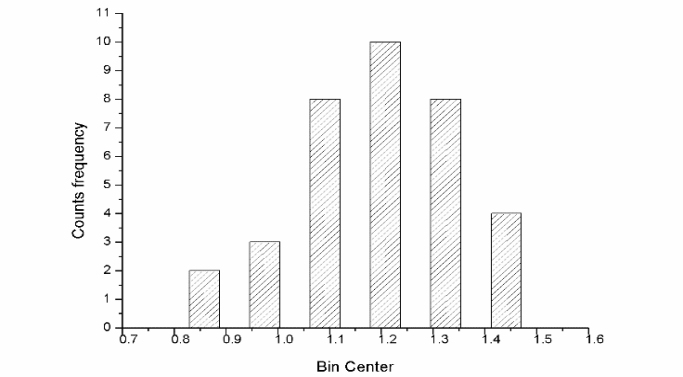

Fig. 1. ED frequency distribution for CG extracted and measured from IM6 sample.

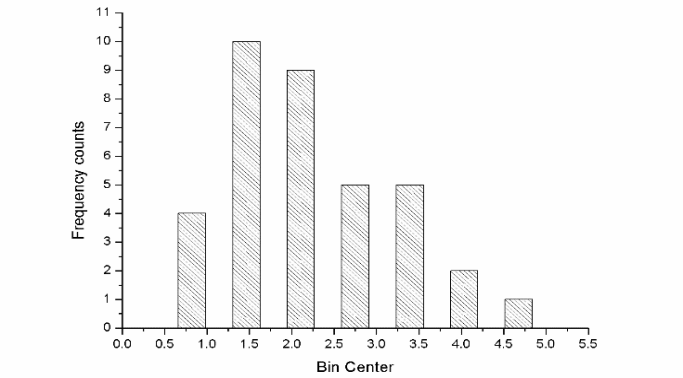

Fig. 2. ED frequency distribution for QI extracted and measured from IM6 sample.

Figure 1, related to the data obtained from CG, shows an ED distribution behavior similar to a Gaussian, while in Figure 2, related to the ED value obtained from QI, a different behavior is observed. In the first case, we can hypothesize that for CG quartz, during mortar preparation and layering, a total bleaching phenomenon was occurred, while QI quartz was subject to partial bleaching phenomenon. This result was found for all measured samples.

However, these diagrams do not take into account uncertainties associated to the equivalent doses. The maximum of the histogram may therefore not coincide with the true archaeological dose, unless the uncertainties are more or less uniform.

Q-Q plot analysis

The Q-Q plots allow evidencing if two sets of data come from the same distribution. A 45-degree angle is considered as reference in the Q-Q plot: if the two data sets come from a common distribution, the points will fall on the related reference line. Figures 3 and 4 show, as example respectively for CG and QI, ED distribution for the IM6 sample.

The quantiles from a theoretical normal distribution are plotted on the horizontal axis and compared to a set of experimental data on the y-axis. For QI (Figure 4), the points are not clustered following the 45-degree line but they show a behaviour suggesting that the data is not normally distributed. For CG (Figure 3), a greater agreement with normal distribution has been found. This result was found for all samples and it confirms the qualitative results obtained by ED frequency distribution.

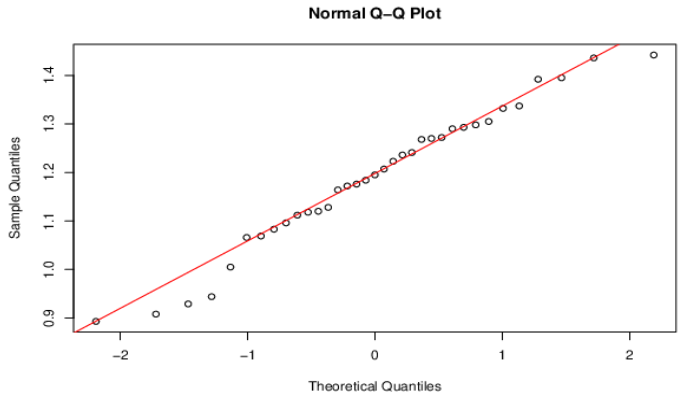

Fig. 3. Q-Q plot for CG extracted and measured from the IM6 sample.

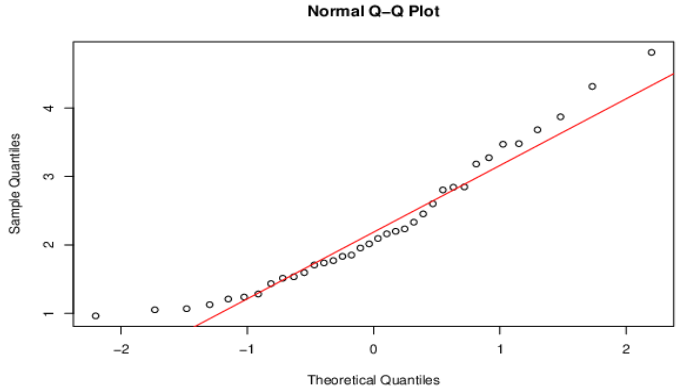

Fig. 4. Q-Q plot for QI extracted and measured from the IM6 sample.

Age Model application

Table 1 shows the results obtained from Shapiro and Wilk's test. For the CG fraction of each sample, the values $W_0>W_0$ (0.5n) and W_0 (p-value)>0.05 data related CG were obtained. These results suggest accepting the null hypothesis and then the experimental data can be considered as a normal distribution. For each sample, related to QI fraction, $W_0<W_0$ (0.5n) and W_0 (p-value) < 0.05 were obtained. In this case, the results suggest a non-normal distribution.

Table 1. Sample ID, size (QI or CG), number (n) of aliquots measured for ED calculation, ED mean and standard deviation (SD) obtnained by ED frequency distribution are listed. The Shapiro and Wilk's parameter (W0) calculated, the Shapiro and Wilk's parameter (W_0 (0.5,n)) tabulated for n ED value were reported. In the last column, the Shapiro and Wilk's parameter W0 considering a p-value 0.05 level of significativity is shown.

Sample ID	Size	n	ED Mean (Gy)	SD (Gy)	W_0	W0(0.5,n)	W0 p-value
IM1	CG	34	1.92	0.29	0.986	0.933	0.932
	QI	37	2.98	0.97	0.929	0.936	0.021
IM6	CG	35	1.19	0.15	0.971	0.934	0.471
	QI	36	2.26	0.78	0.915	0.935	0.010
IM7	CG	35	1.47	0.21	0.982	0.934	0.822
	QI	36	2.34	0.79	0.921	0.935	0.013
IM9	CG	37	5.02	0.56	0.981	0.936	0.766
	QI	36	6.22	2.03	0.927	0.935	0.020

Table 2 shows the ED results obtained from radial plot analysis coupled with CAM for CG data and MAM for QI data.

Based on the results obtained by Shapiro Wilk's tests, in order to determine the best representation of the true archaeological ED, CAM for CG ED data and MAM model for QI ED data were used [32]. Figure 5 and 6 respectively show an example of radial plot analysis for CG and QI fractions for the IM6 sample.

Table 2. Sample ID and the relative granulometric size (QI e CG) are listed according to the Model Age used and the archaeological ED in Gray (Gy) calculated.

Sample ID	Size	Model Age	ED (Gy)
IM1	CG	CAM	1.71±0.12
	QI	MAM	1.48±0.15
IM6	CG	CAM	1.18±0.08
	QI	MAM	1.06± 0.07
IM7	CG	CAM	1.44±0.12
	QI	MAM	1.23±0.19
IM9	CG	CAM	4.91±0.32
	QI	MAM	4.32±0.48

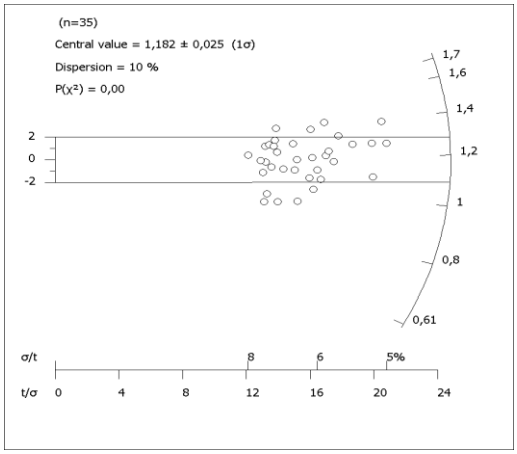

Fig. 5. Radial plot for CG extracted and measured from IM6 sample based on the CAM model.

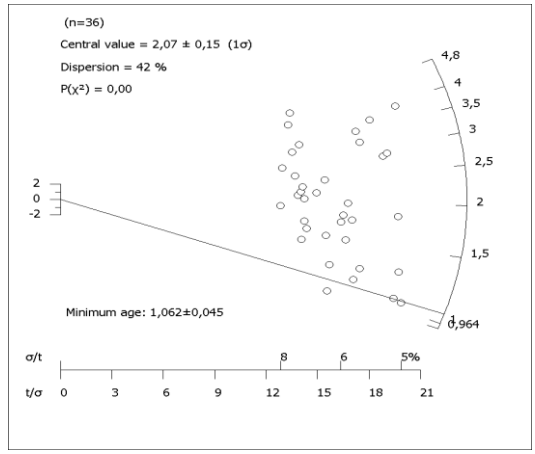

Fig. 6. Radial plot for QI extracted and measured from IM6 sample based on the MAM model.

Conclusions

The paper shows the potential use of a statistical analysis approach based on ED frequency distribution. Statistical knowledge helps to employ the correct analyses and effectively present the results. This is fundamental in the case of historical mortar study for producing reliable data and drawing reasonable conclusions considering the bleaching degree issue that affects the Equivalent Dose data elaboration.

In particular, Q-Q plot and Shapiro-Wilk normality test are used to evaluate bleaching degree of quartz fraction extracted by historical mortars in order to choose the more appropriate age model. The statistical study was useful to evidence the bleaching level associated to manufacturing phase of the mortar. The results show a partial bleaching degree for QI and a total bleaching degree for CG.

The equivalent doses obtained respectively with the MAM method for the QI and CAM for the CG are in good agreement and confirm the goodness of the procedure used.

In the following flow chart (Figure 7) the statistical approach for ED determination in historical mortars dating is shown.

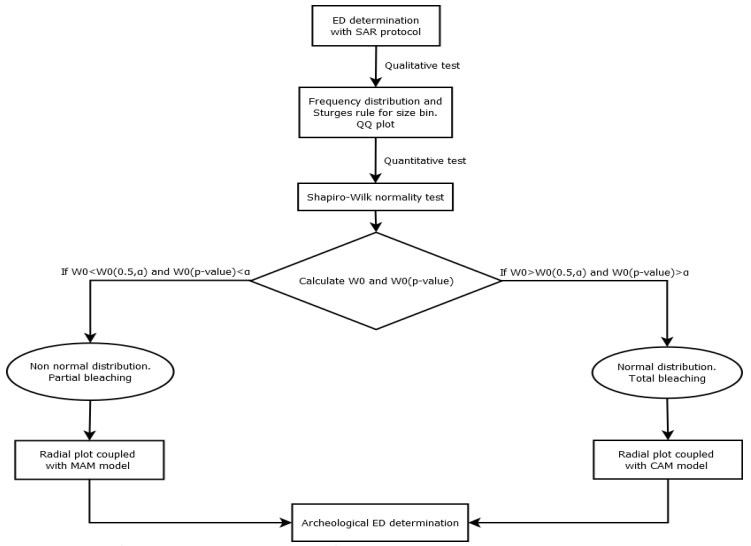

Fig. 7. Flow chart for a statistical approach for ED determination in historical mortars dating.

References

[1] N. Zacharias, B. Mauz, C.T. Michael, *Luminescence quartz dating of lime mortars. A first research approach*, **Radiation Protection Dosimetry** 101, 2002, pp. 379–382.

[2] J.K. Feathers, J. Johnson, S.R. Kembel, *Luminescence Dating of Monumental Stone Architecture at Chavín De Huántar, Perú*, **Journal of Archaeological Method and Theory,** 15, 2008, pp.266–296.

[3] A.M. Gueli, G. Stella, S.O. Troja, G. Burrafato, D. Fontana, G.M. Ristuccia, A.R. Zuccarello, *Historical buildings: luminescence dating of fine grains from bricks and mortar*, **Il Nuovo Cimento B**, 125(5–6), 2010, pp. 719–729.

[4] C. Goedicke, *Dating mortar by optically stimulated luminescence: a feasibility study*, **Geochronometria**, 38, 2011, pp. 42–49.

[5] L. Panzeri, *Mortar and surface dating with optically stimulated luminescence (OSL): innovative techniques for the age determination of buildings*, **Nuovo Cimento C**, 36(4), 2013, pp.205–216.

[6] G. Stella, D. Fontana, A.M. Gueli, S.O. Troja, *Historical mortars dating from OSL signals of fine grain fraction enriched in quartz*, **Geochronometria**, 40(3), 2013, pp.153–164.

[7] P. Urbanová, D. Hourcade, C. Ney, P. Guibert, *Sources of uncertainties in OSL dating of archaeological mortars: the case study of the Roman amphitheatre Palais-Gallien in Bordeaux*, **Radiation Measurements**, 72, 2015, pp.100–110.

[8] P. Urbanová, E. Delaval, P. Dufresne, P. Lanos, P. Guibert, *Multimethod dating comparison of Grimaldi castle foundations in Antibes, France*, **ArchéoSciences-Revue d'archéométrie**, 40, 2016, pp.17–33.

[9] P. Guibert, C. Christophe, P. Urbanová, S. Blain, G. Guérin, *Modeling incomplete and heterogeneous bleaching of mobile grains partially exposed to the light: towards a new tool for single grain OSL dating of poorly bleached mortars*, **Radiation Measurements** 107, 2017, pp.48–57.

[10] P. Urbanová, P. Guibert, *Methodological study on single grain OSL dating of mortars: Comparison of five reference archaeological sites*, **Geochronometria**, 44(1), 2017, pp. 77–97.

[11] G. Stella, L. Almeida, L. Basilio, S. Pasquale, J. Dinis, M. Almeida, A.M. Gueli, *Historical building dating: a multidisciplinary study of the convento of Sao Francisco (Coimbra, Portugal)*, **Geochronometria,** 45, 2018, pp.119-129.

[12] L. Panzeri, M. Cantù, M. Martini, E. Sibilia, *Application of different protocols and age models in OSL dating of earthen mortars*, **Geochronometria**, 44, 2017, pp.341–351.

[13] R.F. Galbraith, R.G. Roberts, G.M. Laslett, H. Yoshida, J.M. Olley, *Optical dating of single and multiple grains of quartz form Jinmium Rock Shelter, northern Australia: Part I, experimental design and statistical models*, **Archaeometry,** 1999, 41, pp.339–364.
[14] L.J. Arnold, R.G. Roberts, *Stochastic modelling of multigrain equivalent dose distributions: Implications for OSL dating of sediment mixtures*, **Quaternary Geochronology,** 4, 2009, pp.204– 230.
[15] A.M. Gueli, V. Garro, M. Liuzzo, G. Margani, S. Pasquale, G. Politi, G. Stella, *Chronology of the roman baths of "Indirizzo" in Catania (Sicily)*, **Proceedings at the IMEKO International Conference on Metrology for Archeology and Cultural Heritage**, 2016, pp.246-250.
[16] A.M. Gueli, V. Garro, M. Liuzzo, G. Margani, S. Pasquale, G. Politi, G. Stella, *Effect of moisture in historical buildings TL ages*, **Measurement,** 118, 2018a, pp.289-297.
[17] R.E. Glaser, *Bartlett's test of homogeneity of variance,* **Encycl. Stat. Sci.,** 1, 1982, p. 189-191.
[18] A.M. Gueli, V. Garro, O. Palio, S. Pasquale, G. Politi, G. Stella, M. Turco, *TL and OSL cross-dating for Valcorrente site in Belpasso (Catania, Italy)*, **European Physical Journal Plus**, 133(12), 2018b, 542.
[19] M.J. Aitken, **Thermoluminescence dating**, 1989, London, Academic Press.
[20] L. Carobene, R. Cirrincione, R. De Rosa, A.M. Gueli, S. Marino, S.O. Troja, *Thermal (TL) and optical stimulated luminescence (OSL) techniques for dating Quaternary colluvial volcaniclastic sediments: An example from the Crati Basin (Northern Calabria)*, **Quaternary International**, 148(1), 2006, pp. 149-164.
[21] P. Guiber, I.K. Bailiff, S. Blain, A.M. Gueli, M. Martini, E. Sibilia, G. Stella, S.O. Troja, *Luminescence dating of architectural ceramics from an early medieval abbey: The St Philbert Intercomparison (Loire Atlantique, France)*, **Radiation Measurements**, 44(5-6), 2009, pp.488-493.
[22] F. Gerardi, A. Smedile, C. Pirrotta, M.S. Barbano, P.M. De Martini, S. Pinzi, A.M. Gueli, G.M. Ristuccia, G. Stella, S.O. Troja, *Geological record of tsunami inundations in Pantano Morghella (south-eastern Sicily) both from near and far-field sources*, **Nat. Hazards Earth Syst. Sci.,** 12, 2012, pp. 1185–1200.
[23] G. Stella, D. Fontana, A.M. Gueli, S.O. Troja, *Different approaches to date bricks from historical buildings*, **Geochronometria**, 41(3), 2014, pp.256–264.
[24] J.H. Choi, A.S. Murray, M. Jain, C.S. Cheong, H.W. Chang, *Luminescence dating of well-sorted marine terrace sediments on the southeastern coast of Korea*, **Quaternary Science Reviews,** 22, 2003, pp.407–421.
[25] A.S. Murray, A.G. Wintle, *Luminescence dating of quartz using an improved single-aliquot regenerative-dose protocol*, **Radiation Measurements**, 32(1), 2000, pp.57-73.
[26] A.S. Murray, A.G. Wintle, *The single aliquot regenerative dose protocol: potential for improvements in reliability*, **Radiation Measurements**, 37, 2003, pp.377–381.
[27] M.J. Aitken, **Introduction to Optical Dating: The Dating of Quaternary Sediments by the Use of Photonstimulated Luminescence**, 1998, Oxford University Press.
[28] L. Bøtter-Jensen, *Luminescence techniques: instrumentation and methods*, **Radiation Measurements**, 27, 1997, pp.749–768.
[29] L. Bøtter-Jensen, E. Bulur, G.A.T. Duller, A.S. Murray, *Advances in luminescence instrument systems*, **Radiation Measurements**, 32, 2000, pp.523–528.
[30] R.J. Hyndman, *Highest density forecast regions for non-linear and non-normal time series models*, **Journal of Forecasting**, 14, 1995, pp.431-441.
[31] S.S. Shapiro, M.B. Wilk *A analysis of variance test for normality (complete samples)*, **Biometrika**, 52, 1965, pp.591–611.
[32] P. Vermeesch, *Radial Plotter: a Java application for fission track, luminescence and other radial plots*, **Radiation Measurements**, 44, 2009, pp.409–410.

Received: January 4, 2020
Accepted: March 28, 2020